

The POG Technique for Modeling Planetary Gears and Hybrid Automotive Systems

Roberto Zanasi

Information Engineering Department
University of Modena e Reggio Emilia
Via Vignolese 905
41100 Modena, Italy
roberto.zanasi@unimore.it

Federica Grossi

Information Engineering Department
University of Modena e Reggio Emilia
Via Vignolese 905
41100 Modena, Italy
federica.grossi@unimore.it

Abstract—In this paper the Power-Oriented Graphs (POG) technique is used for modeling planetary gears and hybrid automotive systems. Some basic properties of the POG technique are firstly given. An extended dynamic model of a planetary gear with internal elasticity is presented. Then a POG congruent state space transformation is used to transform and reduce the system when the elasticities or the inertias go to zero. The obtained reduced model is used as central element of an hybrid automotive power structure (endothermic engine, multi-phase synchronous motor and vehicle dynamics). Simulation results will be reported in the final full paper.

I. INTRODUCTION

Nowadays, the planetary gears are key elements for the design of new hybrid power structures in the automotive area. In this paper, some different dynamic models for these systems are obtained using the the POG modeling technique.

(References and a detailed description of the work done in the literature in this field will be given in the final full paper).

The paper is organized as follows: Sec. II describes the basic properties of the POG modeling technique. Sec. III and Sec. IV show, respectively, the POG dynamic models of full and reduced planetary gears, and of an hybrid automotive power structure composed by an endothermic engine, a multi-phase synchronous motor and the vehicle dynamics. Finally, in Sec. V some simulation results are reported.

II. POWER-ORIENTED GRAPHS BASIC PRINCIPLES

The Power-Oriented Graphs technique, see [1] and [2], is suitable for modeling physical systems. The POG block schemes are normal block diagrams combined with a particular modular structure essentially based on the use of the two blocks shown in Fig. 1.a and Fig. 1.b: the *elaboration block* (e.b.) stores and/or dissipates energy (i.e. springs, masses, dampers, capacities, inductances, resistances, etc.); the *connection block* (c.b.) redistributes the power within the system without storing nor dissipating energy (i.e. any type of gear reduction, transformers, etc.). The e.b. and the c.b. are suitable for representing both scalar and vectorial systems. In the vectorial case, $\mathbf{G}(s)$ and \mathbf{K} are matrices: $\mathbf{G}(s)$ is always a square matrix composed by positive real transfer functions; matrix \mathbf{K} can also be rectangular. The circle present in the e.b. is a summation element and the black spot represents a minus

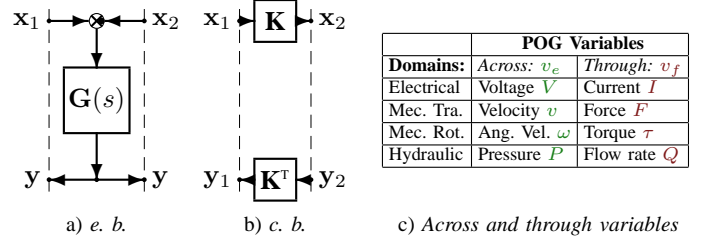


Figure 1. POG basic blocks and variables: a) *elaboration block*; b) *connection block*; c) *across and through variables*.

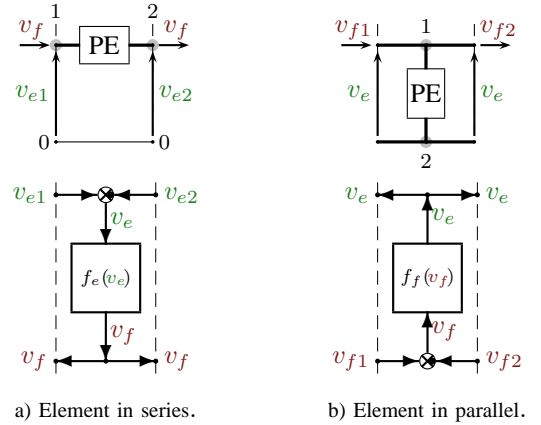


Figure 2. POG representations of Physical Elements (PE): a) connected in series (inputs v_{e1} , v_{e2}); b) connected in parallel (inputs v_{f1} , v_{f2}).

sign that multiplies the entering variable. The main feature of the Power-Oriented Graphs is to keep a direct correspondence between the dashed sections of the graphs and real power sections of the modeled systems: the scalar product $\mathbf{x}^T \mathbf{y}$ of the two *power vectors* \mathbf{x} and \mathbf{y} involved in each dashed line of a power-oriented graph, see Fig. 1, has the physical meaning of *the power flowing through that particular section*. The Bond Graphs technique, see [3], is based on the same idea, but it uses a different and specific graphical representation.

The main energetic domains encountered in modeling physical systems are the electrical, the mechanical (translational and rotational) and the hydraulic, see Fig. 1.c. Each energetic

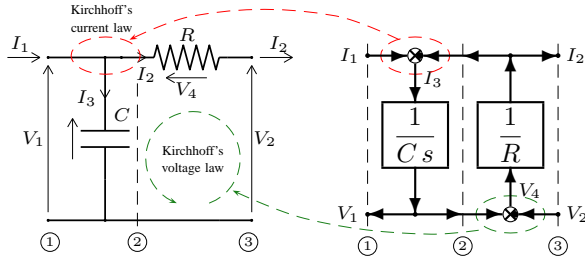


Figure 3. POG modeling of an electrical RC circuit.

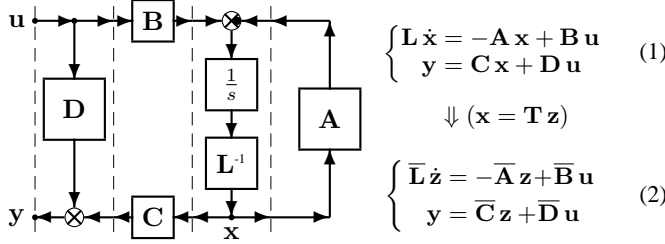


Figure 4. POG block scheme of a generic dynamic system.

domain is characterized by two *power variables*: an *across-variable* v_e defined between two points (i.e. the voltage V), and a *through-variable* v_f defined in each point of the space (i.e. the current I). Each Physical Element (PE) interacts with the external world through the power sections associated to its terminals. A Physical Element is connected *in series* when its terminals share the same through-variable v_f : see the physical element and the corresponding POG scheme in Fig. 2.a. A Physical Element is connected *in parallel* when its terminals share the same across-variable v_e : see the physical element and the POG scheme in Fig. 2.b. An example of POG modeling where a C parallel element is connected with an R series element is shown in Fig. 3. There is a direct correspondence between physical power sections and dashed sections in the POG model. Note: the summation elements present in the elaboration blocks are a mathematical description of the current and voltage Kirchhoff's laws applied to the considered electrical system.

Another important property of the POG technique is the direct correspondence between the POG block schemes and the corresponding state space dynamic equations. For example, the POG scheme shown in Fig. 4 can be represented by the state space equations (1) where the *energy matrix* \mathbf{L} is symmetric and positive definite: $\mathbf{L} = \mathbf{L}^T > 0$. For the POG systems described in form (1) it can be shown that when $\mathbf{D} = 0$ it is $\mathbf{C} = \mathbf{B}^T$. When an eigenvalue of matrix \mathbf{L} tends to zero (or to infinity), system (1) degenerates towards a lower dimension dynamic system. In this case, the dynamic model of the “reduced” system, see (2), can be directly obtained from (1) using a simple “congruent” transformation $\mathbf{x} = \mathbf{T}\mathbf{z}$ where, if \mathbf{T} is constant, $\bar{\mathbf{L}} = \mathbf{T}^T \mathbf{L} \mathbf{T}$, $\bar{\mathbf{A}} = \mathbf{T}^T \mathbf{A} \mathbf{T}$, $\bar{\mathbf{B}} = \mathbf{T}^T \mathbf{B}$, $\bar{\mathbf{C}} = \mathbf{C} \mathbf{T}$ and $\bar{\mathbf{D}} = \mathbf{D}$. The POG scheme of Fig. 4 can also be easily input-output inverted, both graphically and mathematically, as shown in Fig. 5 where $\tilde{\mathbf{L}} = \mathbf{L}$, $\tilde{\mathbf{A}} = \mathbf{A} + \mathbf{B} \mathbf{D}^{-1} \mathbf{C}$,

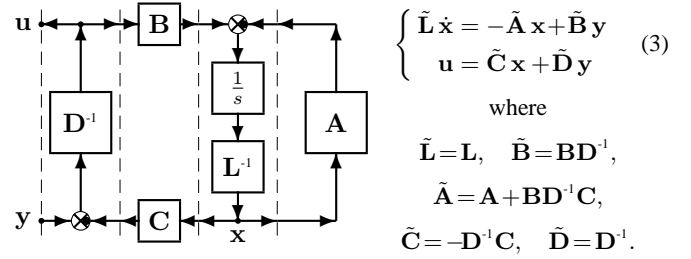


Figure 5. POG block scheme of the input-output inverted system.

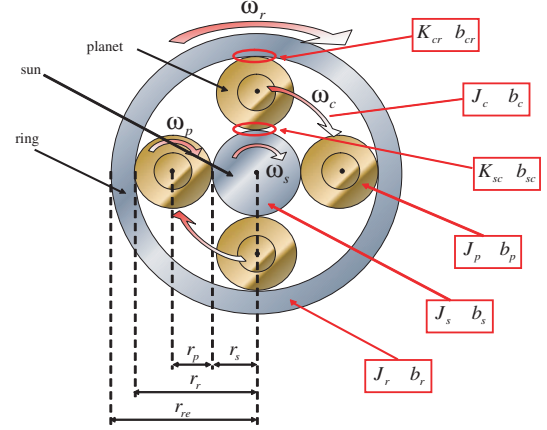


Figure 6. Planetary gear and related parameters.

$\tilde{\mathbf{B}} = \mathbf{B} \mathbf{D}^{-1}$, $\tilde{\mathbf{C}} = -\mathbf{D}^{-1} \mathbf{C}$ and $\tilde{\mathbf{D}} = \mathbf{D}^{-1}$ are the matrices of the inverted system (3).

III. POG MODELING OF A PLANETARY GEAR

Let us consider the planetary gear shown in Fig. 6 together with the main parameters of the system. The extended POG dynamic model of the considered planetary gear is shown in the upper part of Fig. 7: the carrier, the planets and the ring interact each other through the two elastic elements K_{cr} and K_{sc} . The corresponding state space dynamic equations are shown in lower part of Fig. 7:

$$\bar{\mathbf{L}} \dot{\bar{\mathbf{x}}} = -\bar{\mathbf{A}} \bar{\mathbf{x}} + \bar{\mathbf{B}} \mathbf{u}, \quad \mathbf{y} = \bar{\mathbf{B}}^T \bar{\mathbf{x}} \quad (5)$$

The POG linear systems described in form (5) satisfy the following properties:

1) the energy E_s stored in the system and the dissipating power P_d are quadratic functions of matrices $\bar{\mathbf{L}}$ and $\bar{\mathbf{A}}_s$, respectively:

$$E_s = \frac{1}{2} \bar{\mathbf{x}}^T \bar{\mathbf{L}} \bar{\mathbf{x}}, \quad P_d = \bar{\mathbf{x}}^T \bar{\mathbf{A}}_s \bar{\mathbf{x}}$$

where $\bar{\mathbf{A}}_s = (\bar{\mathbf{A}} + \bar{\mathbf{A}}^T)/2$ is the symmetric part of the *power matrix* $\bar{\mathbf{A}}$. The skew-symmetric part $\bar{\mathbf{A}}_w = (\bar{\mathbf{A}} - \bar{\mathbf{A}}^T)/2$ of matrix $\bar{\mathbf{A}}$ represents the power redistribution within the system. One can easily verify that all the dissipating parameters of the system appear only in matrix $\bar{\mathbf{A}}_s$, while matrix $\bar{\mathbf{A}}_w$ is completely characterized by all the connection parameters; 2) all the loops of the POG schemes contain always an “odd” number of minus signs “-” (i.e. the black spots present in the

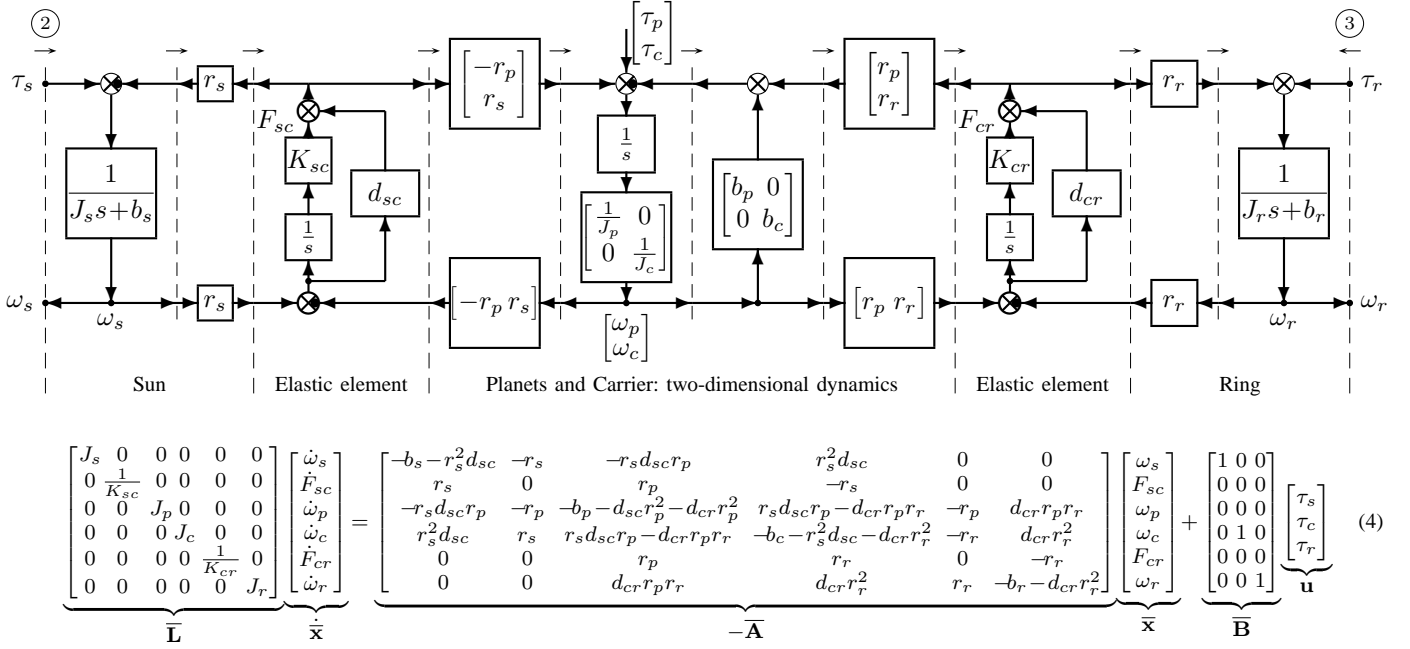


Figure 7. The POG block diagram and the POG state space equations of the considered planetary gear: the sun, the planets-carrier and the ring interact through elastic elements. The considered inputs are: τ_s , τ_c and τ_r .

summation blocks);

3) the direction of the power flowing through a section is positive if an “even” number of signs “-” is present along all the paths which link the input and the output of the section. Note, for example, that in Fig. 7 the power is entering the system in both sections ② and ③.

A. Reduced inertial model

For certain applications the POG model of Fig. 7 can be too much detailed. In these cases it can be of interest to find the reduced model when, for example, the stiffness coefficients K_{cr} and K_{sc} tend to infinity. Applying to system (5) the following congruent transformation:

$$\bar{x} = T_1 x, \quad \text{where} \quad T_1 = \begin{bmatrix} 1 & 0 & 0 & 0 & 0 & 0 \\ 0 & 0 & 0 & 0 & 0 & 1 \\ 0 & 0 & 1 & 0 & 0 & 0 \\ 0 & 1 & 0 & 0 & 0 & 0 \\ 0 & 0 & 0 & 0 & 1 & 0 \\ 0 & 0 & 0 & 1 & 0 & 0 \end{bmatrix}.$$

one obtains the following transformed system:

$$\underbrace{\begin{bmatrix} J_1 & 0 & 0 \\ 0 & J_2 & 0 \\ 0 & 0 & 0 \end{bmatrix}}_{\bar{L}} \underbrace{\begin{bmatrix} \dot{x}_1 \\ \dot{x}_2 \\ \dot{x}_3 \end{bmatrix}}_{\dot{x}} = \underbrace{\begin{bmatrix} A_{11} & A_{12} & A_{13} \\ A_{21} & A_{22} & A_{23} \\ A_{31} & A_{32} & 0 \end{bmatrix}}_{-\bar{A}} \underbrace{\begin{bmatrix} x_1 \\ x_2 \\ x_3 \end{bmatrix}}_x + \underbrace{\begin{bmatrix} B_1 \\ B_2 \\ 0 \end{bmatrix}}_{\bar{B}} u \quad (6)$$

where $x = T_1^T \bar{x}$, $\bar{L} = T_1^T L T_1$, $\bar{B} = T_1^T B$, $\bar{A} = T_1^T A T_1$, $y = B^T x$ and where:

$$x_1 = \begin{bmatrix} \omega_s \\ \omega_c \end{bmatrix}, \quad x_2 = \begin{bmatrix} \omega_p \\ \omega_r \end{bmatrix}, \quad x_3 = \begin{bmatrix} F_{cr} \\ F_{sc} \end{bmatrix}, \quad J_1 = \begin{bmatrix} J_s & 0 \\ 0 & J_c \end{bmatrix}, \quad J_2 = \begin{bmatrix} J_p & 0 \\ 0 & J_r \end{bmatrix},$$

$$B_1 = \begin{bmatrix} 1 & 0 \\ 0 & 1 \end{bmatrix}, \quad B_2 = \begin{bmatrix} 0 & 0 \\ 0 & 1 \end{bmatrix}, \quad A_{11} = \begin{bmatrix} -b_s - r_s^2 d_{sc} & r_s^2 d_{sc} \\ r_s^2 d_{sc} & -b_c - r_s^2 d_{sc} - d_{cr} r_r^2 \end{bmatrix},$$

$$A_{12} = \begin{bmatrix} -r_s d_{sc} r_p & 0 \\ r_s d_{sc} r_p - d_{cr} r_p r_r & d_{cr} r_r^2 \end{bmatrix}, \quad A_{13} = \begin{bmatrix} 0 & -r_s \\ -r_r & r_s \end{bmatrix}, \quad A_{31} = \begin{bmatrix} 0 & r_r \\ r_s & -r_s \end{bmatrix},$$

$$A_{21} = \begin{bmatrix} -r_s d_{sc} r_p & r_s d_{sc} r_p - d_{cr} r_p r_r \\ 0 & d_{cr} r_r^2 \end{bmatrix}, \quad A_{23} = \begin{bmatrix} -r_p & -r_p \\ r_r & 0 \end{bmatrix},$$

$$A_{22} = \begin{bmatrix} -b_p - d_{sc} r_p^2 - d_{cr} r_p^2 & d_{cr} r_p r_r \\ d_{cr} r_p r_r & -b_r - d_{cr} r_r^2 \end{bmatrix}, \quad A_{32} = \begin{bmatrix} r_p & -r_r \\ r_p & 0 \end{bmatrix}.$$

The last equation of system (6) shows an algebraic relation between the state variables: $A_{31} x_1 + A_{32} x_2 = 0$. Since matrix A_{32} is invertible, vector x_2 can be expressed as:

$$x_2 = \begin{bmatrix} \omega_p \\ \omega_r \end{bmatrix} = -A_{32}^{-1} A_{31} x_1 = \begin{bmatrix} -\frac{r_s}{r_p} & \frac{r_s}{r_p} \\ -\frac{r_s}{r_r} & 1 + \frac{r_s}{r_r} \end{bmatrix} \begin{bmatrix} \omega_s \\ \omega_c \end{bmatrix}$$

Applying the following “rectangular” transformation:

$$x = T_2 x_1 \quad \text{where} \quad T_2 = \begin{bmatrix} I_2 \\ -A_{32}^{-1} A_{31} \\ 0 \end{bmatrix} = \begin{bmatrix} 1 & 0 \\ 0 & 1 \\ -\frac{r_s}{r_p} & \frac{r_s}{r_p} \\ -\frac{r_s}{r_r} & 1 + \frac{r_s}{r_r} \\ 0 & 0 \\ 0 & 0 \end{bmatrix}$$

to system (6), one obtains the following second order transformed and reduced system:

$$L_r \dot{x}_1 = -A_r x_1 + B_r u, \quad y = B_r^T x_1, \quad (7)$$

where $L_r = T_2^T L T_2$, $A_r = T_2^T A T_2$ and $B_r = T_2^T B$ are:

$$L_r = \begin{bmatrix} J_s + \frac{r_s^2}{r_p^2} J_p + \frac{r_s^2}{r_r^2} J_r & -\frac{r_s^2}{r_p^2} J_p - \frac{r_s}{r_r} \left(1 + \frac{r_s}{r_r}\right) J_r \\ -\frac{r_s^2}{r_p^2} J_p - \frac{r_s}{r_r} \left(1 + \frac{r_s}{r_r}\right) J_r & J_c + \frac{r_s^2}{r_p^2} J_p + \left(1 + \frac{r_s}{r_r}\right)^2 J_r \end{bmatrix}$$

$$A_r = \begin{bmatrix} b_s + \frac{r_s^2}{r_p^2} b_p + \frac{r_s^2}{r_r^2} b_r & -\frac{r_s^2}{r_p^2} b_p - \frac{r_s}{r_r} \left(1 + \frac{r_s}{r_r}\right) b_r \\ -\frac{r_s^2}{r_p^2} b_p - \frac{r_s}{r_r} \left(1 + \frac{r_s}{r_r}\right) b_r & b_c + \frac{r_s^2}{r_p^2} b_p + \left(1 + \frac{r_s}{r_r}\right)^2 b_r \end{bmatrix}$$

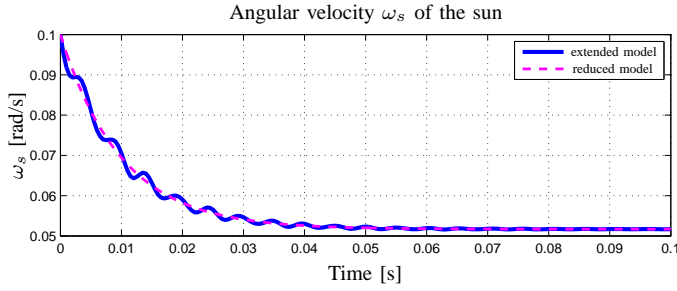


Figure 8. Simulative comparison between the extended (blue solid line) and the reduced (magenta dashed line) model of the planetary gear.

$$\mathbf{B}_r = \begin{bmatrix} 1 & 0 & -\frac{r_s}{r_r} \\ 0 & 1 & 1 + \frac{r_s}{r_r} \end{bmatrix}, \quad \mathbf{x}_1 = \begin{bmatrix} \omega_s \\ \omega_c \end{bmatrix}, \quad \mathbf{y} = \begin{bmatrix} \omega_s \\ \omega_c \\ \omega_r \end{bmatrix}$$

Note that the possibility of using a “rectangular” matrix \mathbf{T}_2 for transforming and reducing a dynamical system is a “specific characteristics” of the POG techniques and it holds only for system described in the POG form (1). A simulative comparison between the extended model (4) and the reduced model (9) of the planetary gear is shown in Fig. 8. The parameters used in simulation are (SI international units): sun parameters $[J_s, b_s, r_s] = [0.0495, 4.9459, 0.1019]$; ring parameters $[J_r, b_r, r_r] = [2.1803, 218.0260, 0.2483]$; carrier parameters $[J_c, b_c] = [0.9290, 92.8975]$; planet parameters $[J_p, b_p, r_p] = [0.0812, 8.1228, 0.0732]$; stiffness parameters $[K_{sc}, d_{sc}] = [K_{cr}, d_{cr}] = [10^7, 10]$; initial conditions $[\omega_s(0), \omega_c(0), \omega_r(0)] = [0.1, -0.2, -0.323]$ rad/s; constant external torques $[\tau_s, \tau_c, \tau_r] = [0, 4, 0]$ Nm. With different choices of matrix \mathbf{T}_1 it is possible to obtain different but equivalent reduced systems, similar to (9), with different state variables in vector \mathbf{x}_1 , for example $\mathbf{x}_1 = [\omega_s, \omega_r]^T$, $\mathbf{x}_1 = [\omega_r, \omega_c]^T$, etc.

B. Reduced elastic model

Using the POG reduction technique it is also possible to obtain from (4) the reduced elastic model when inertias J_s , J_c and J_r go to zero. Applying to system (5) the following congruent transformation:

$$\bar{\mathbf{x}} = \mathbf{T}_3 \mathbf{z}, \quad \text{where} \quad \mathbf{T}_3 = \begin{bmatrix} 0 & 0 & 0 & 1 & 0 & 0 \\ 1 & 0 & 0 & 0 & 0 & 0 \\ 0 & 1 & 0 & 0 & 0 & 0 \\ 0 & 0 & 0 & 0 & 1 & 0 \\ 0 & 0 & 1 & 0 & 0 & 0 \\ 0 & 0 & 0 & 0 & 0 & 1 \end{bmatrix}.$$

with the additional constraint $J_s = J_c = J_r = 0$ one obtains a transformed system in the form:

$$\underbrace{\begin{bmatrix} \mathbf{L}_1 & 0 \\ 0 & 0 \end{bmatrix}}_{\mathbf{L}} \underbrace{\begin{bmatrix} \dot{\mathbf{z}}_1 \\ \dot{\mathbf{z}}_2 \end{bmatrix}}_{\dot{\mathbf{z}}} = \underbrace{\begin{bmatrix} \mathbf{A}_{11} & \mathbf{A}_{12} \\ \mathbf{A}_{21} & \mathbf{A}_{22} \end{bmatrix}}_{-\mathbf{A}} \underbrace{\begin{bmatrix} \mathbf{z}_1 \\ \mathbf{z}_2 \end{bmatrix}}_{\mathbf{z}} + \underbrace{\begin{bmatrix} \mathbf{B}_1 \\ \mathbf{B}_2 \end{bmatrix}}_{\mathbf{B}} \mathbf{u}, \quad \mathbf{y} = \mathbf{C} \mathbf{z} + \mathbf{D} \mathbf{u}, \quad (8)$$

where $\mathbf{z} = \mathbf{T}_1^T \bar{\mathbf{x}}$, $\mathbf{L} = \mathbf{T}_3^T \bar{\mathbf{L}} \mathbf{T}_3$, $\mathbf{A} = \mathbf{T}_3^T \bar{\mathbf{A}} \mathbf{T}_3$, $\mathbf{B} = \mathbf{T}_3^T \bar{\mathbf{B}}$, $\mathbf{C} = [\mathbf{C}_1, \mathbf{C}_2] = \mathbf{B}^T = [\mathbf{B}_1^T, \mathbf{B}_2^T]$, $\mathbf{D} = 0$ and where:

$$\mathbf{z}_1 = \begin{bmatrix} F_{sc} \\ \omega_p \\ F_{cr} \end{bmatrix}, \quad \mathbf{z}_2 = \begin{bmatrix} \omega_s \\ \omega_c \\ \omega_r \end{bmatrix}, \quad \mathbf{L}_1 = \begin{bmatrix} \frac{1}{K_{sc}} & 0 & 0 \\ 0 & J_p & 0 \\ 0 & 0 & \frac{1}{K_{cr}} \end{bmatrix},$$

$$\mathbf{A}_{11} = \begin{bmatrix} 0 & r_p & 0 \\ -r_p & -d_{sc} r_p^2 - r_p^2 d_{cr} - b_p & -r_p \\ 0 & r_p & 0 \end{bmatrix}, \quad \mathbf{B}_1 = \begin{bmatrix} 0 & 0 & 0 \\ 0 & 0 & 0 \\ 0 & 0 & 0 \end{bmatrix},$$

$$\mathbf{A}_{12} = \begin{bmatrix} r_s & -r_s & 0 \\ -r_s d_{sc} r_p & r_s d_{sc} r_p - r_p r_r d_{cr} & r_p r_r d_{cr} \\ 0 & r_r & -r_r \end{bmatrix}, \quad \mathbf{B}_2 = \begin{bmatrix} 1 & 0 & 0 \\ 0 & 1 & 0 \\ 0 & 0 & 1 \end{bmatrix},$$

$$\mathbf{A}_{21} = \begin{bmatrix} -r_s & -r_s d_{sc} r_p & 0 \\ r_s & r_s d_{sc} r_p - r_p r_r d_{cr} & -r_r \\ 0 & r_p r_r d_{cr} & r_r \end{bmatrix}, \quad \mathbf{D} = \begin{bmatrix} 0 & 0 & 0 \\ 0 & 0 & 0 \\ 0 & 0 & 0 \end{bmatrix},$$

$$\mathbf{A}_{22} = \begin{bmatrix} -b_s - r_s^2 d_{sc} & r_s^2 d_{sc} & 0 \\ r_s^2 d_{sc} & -b_c - r_s^2 d_{sc} - r_r^2 d_{cr} & r_r^2 d_{cr} \\ 0 & r_r^2 d_{cr} & -b_r - r_r^2 d_{cr} \end{bmatrix}.$$

The last equation of system (8) shows the following algebraic relation between the state and the input variables:

$$\mathbf{A}_{21} \mathbf{z}_1 + \mathbf{A}_{22} \mathbf{z}_2 + \mathbf{B}_2 \mathbf{u} = 0$$

Since matrix \mathbf{A}_{22} is invertible, vector \mathbf{z}_2 can be expressed as:

$$\mathbf{z}_2 = -\mathbf{A}_{22}^{-1} \mathbf{A}_{21} \mathbf{z}_1 - \mathbf{A}_{22}^{-1} \mathbf{B}_2 \mathbf{u}$$

Applying the following transformation:

$$\mathbf{z} = \underbrace{\begin{bmatrix} \mathbf{I}_2 \\ -\mathbf{A}_{22}^{-1} \mathbf{A}_{21} \end{bmatrix}}_{\mathbf{T}_z} \mathbf{z}_1 + \underbrace{\begin{bmatrix} 0 \\ -\mathbf{A}_{22}^{-1} \mathbf{B}_2 \end{bmatrix}}_{\mathbf{T}_u} \mathbf{u}$$

to system $\mathbf{L} \dot{\mathbf{z}} = -\mathbf{A} \mathbf{z} + \mathbf{B} \mathbf{u}$ and $\mathbf{y} = \mathbf{C} \mathbf{z} + \mathbf{D} \mathbf{u}$ given in (8), one obtains the following reduced system (note: $\mathbf{L} \mathbf{T}_u = 0$):

$$\begin{cases} \mathbf{T}_z^T \mathbf{L} \mathbf{T}_z \dot{\mathbf{z}}_1 = -\mathbf{T}_z^T \mathbf{A} \mathbf{T}_z \mathbf{z}_1 + \mathbf{T}_z^T (\mathbf{B} - \mathbf{A} \mathbf{T}_u) \mathbf{u} \\ \mathbf{y} = \mathbf{C} \mathbf{T}_z \mathbf{z}_1 + (\mathbf{D} + \mathbf{C} \mathbf{T}_u) \mathbf{u} \end{cases}$$

that in compact form is:

$$\mathbf{L}_e \dot{\mathbf{z}}_1 = -\mathbf{A}_e \mathbf{z}_1 + \mathbf{B}_e \mathbf{u}, \quad \mathbf{y} = \mathbf{C}_e^T \mathbf{z}_1 + \mathbf{D}_e^T \mathbf{u} \quad (9)$$

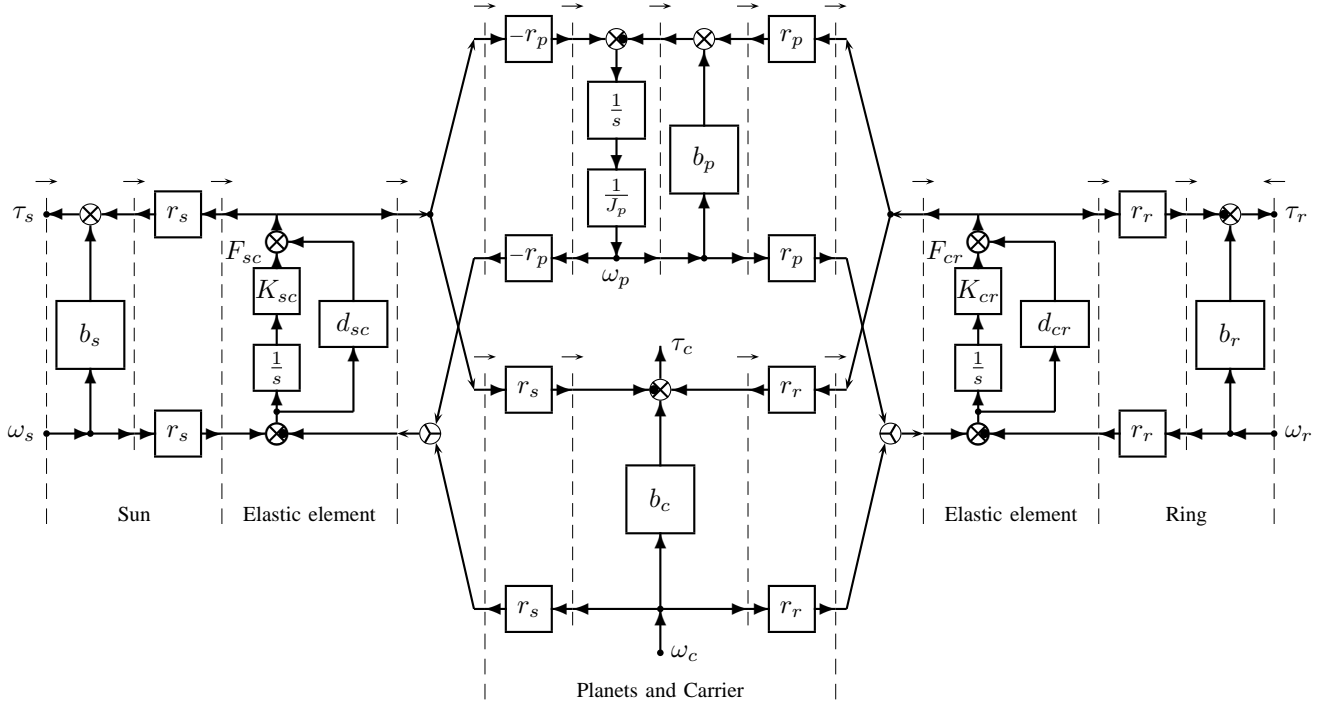
where matrices \mathbf{L}_e , \mathbf{A}_e , \mathbf{B}_e , \mathbf{C}_e and \mathbf{D}_e are the following:

$$\begin{aligned} \mathbf{L}_e &= \mathbf{T}_z^T \mathbf{L} \mathbf{T}_z = \mathbf{L}_1 \\ -\mathbf{A}_e &= -\mathbf{T}_z^T \mathbf{A} \mathbf{T}_z = \mathbf{A}_{11} - \mathbf{A}_{12} \mathbf{A}_{22}^{-1} \mathbf{A}_{21} \\ \mathbf{B}_e &= \mathbf{T}_z^T (\mathbf{B} - \mathbf{A} \mathbf{T}_u) = \mathbf{B}_1 - \mathbf{A}_{12} \mathbf{A}_{22}^{-1} \mathbf{B}_2 \\ \mathbf{C}_e &= \mathbf{C} \mathbf{T}_z = \mathbf{C}_1 - \mathbf{C}_2 \mathbf{A}_{22}^{-1} \mathbf{A}_{21} \\ \mathbf{D}_e &= \mathbf{D} + \mathbf{C} \mathbf{T}_u = \mathbf{D} - \mathbf{C}_2 \mathbf{A}_{22}^{-1} \mathbf{B}_2 \end{aligned}$$

Since matrix \mathbf{D}_e is invertible, system (9) can be input-output inverted using the relations shown in Fig. 5. The state space equations $\tilde{\mathbf{L}}_e \dot{\tilde{\mathbf{x}}} = -\tilde{\mathbf{A}}_e \tilde{\mathbf{x}} + \tilde{\mathbf{B}}_e \tilde{\mathbf{u}}$ and $\tilde{\mathbf{y}} = \tilde{\mathbf{C}}_e \tilde{\mathbf{x}} + \tilde{\mathbf{D}}_e \tilde{\mathbf{u}}$ of the inverted-reduced system are shown in (10) in the lower part of Fig. 9 where:

$$\begin{aligned} \tilde{\mathbf{L}}_e &= \mathbf{L}_e, \quad \tilde{\mathbf{A}}_e = \mathbf{A}_e + \mathbf{B}_e \mathbf{D}_e^{-1} \mathbf{C}_e, \quad \tilde{\mathbf{B}}_e = \mathbf{B}_e \mathbf{D}_e^{-1}, \quad \tilde{\mathbf{C}}_e = -\mathbf{D}_e^{-1} \mathbf{C}_e, \\ \tilde{\mathbf{x}} &= \mathbf{z}_1, \quad \tilde{\mathbf{u}} = \mathbf{y} = [\omega_s, \omega_c, \omega_r]^T, \quad \tilde{\mathbf{y}} = \mathbf{u} = [\tau_s, \tau_c, \tau_r]^T, \quad \tilde{\mathbf{D}}_e = \mathbf{D}_e^{-1}. \end{aligned}$$

A POG graphical representation of this inverted-reduced system is shown in the upper part of Fig. 9.



$$\begin{aligned}
 \underbrace{\begin{bmatrix} \frac{1}{K_{sc}} & 0 & 0 \\ 0 & J_p & 0 \\ 0 & 0 & \frac{1}{K_{cr}} \end{bmatrix}}_{\tilde{\mathbf{L}}_e} \underbrace{\begin{bmatrix} \dot{F}_{sc} \\ \dot{\omega}_p \\ \dot{F}_{cr} \end{bmatrix}}_{\dot{\tilde{\mathbf{x}}}} &= \underbrace{\begin{bmatrix} 0 & r_p & 0 \\ -r_p & -r_p^2 d_{sc} - b_p - r_p^2 d_{cr} & -r_p \\ 0 & r_p & 0 \end{bmatrix}}_{-\tilde{\mathbf{A}}_e} \underbrace{\begin{bmatrix} F_{sc} \\ \omega_p \\ F_{cr} \end{bmatrix}}_{\tilde{\mathbf{x}}} + \underbrace{\begin{bmatrix} r_s & -r_s & 0 \\ -r_s d_{sc} r_p & r_s d_{sc} r_p - r_r d_{cr} r_p & r_r d_{cr} r_p \\ 0 & r_r & -r_r \end{bmatrix}}_{\tilde{\mathbf{B}}_e} \underbrace{\begin{bmatrix} \omega_s \\ \omega_c \\ \omega_r \end{bmatrix}}_{\tilde{\mathbf{u}}} \\
 \underbrace{\begin{bmatrix} \tau_s \\ \tau_c \\ \tau_r \end{bmatrix}}_{\tilde{\mathbf{y}}} &= \underbrace{\begin{bmatrix} r_s & r_s d_{sc} r_p & 0 \\ -r_s & -r_s d_{sc} r_p + r_r d_{cr} r_p & r_r \\ 0 & -r_r d_{cr} r_p & -r_r \end{bmatrix}}_{\tilde{\mathbf{C}}_e} \underbrace{\begin{bmatrix} F_{sc} \\ \omega_p \\ F_{cr} \end{bmatrix}}_{\tilde{\mathbf{x}}} + \underbrace{\begin{bmatrix} b_s + r_s^2 d_{sc} & -r_s^2 d_{sc} & 0 \\ -r_s^2 d_{sc} & b_c + r_s^2 d_{sc} + r_r^2 d_{cr} & -r_r^2 d_{cr} \\ 0 & -r_r^2 d_{cr} & b_r + r_r^2 d_{cr} \end{bmatrix}}_{\tilde{\mathbf{D}}_e} \underbrace{\begin{bmatrix} \omega_s \\ \omega_c \\ \omega_r \end{bmatrix}}_{\tilde{\mathbf{u}}}
 \end{aligned} \quad (10)$$

Figure 9. POG block diagram and POG state space equations of the reduced planetary gear when $J_s = J_c = J_r = 0$ and the velocities are the inputs.

C. Reduced dissipative models

A first dissipative static model of the considered system can be obtained from the inertial model (9) when $J_s = J_c = J_p = J_r = 0$, that is when $\mathbf{L}_r = 0$:

$$\mathbf{x}_1 = \mathbf{A}_r^{-1} \mathbf{B}_r \mathbf{u}, \quad \rightarrow \quad \mathbf{y} = \mathbf{D}_{s1} \mathbf{u} = \mathbf{B}_r^T \mathbf{A}_r^{-1} \mathbf{B}_r \mathbf{u}. \quad (11)$$

Matrix \mathbf{D}_{s1} is singular and therefore all the torque vectors $\mathbf{u} = [\tau_s, \tau_c, \tau_r]^T$ which belong to the kernel of matrix \mathbf{B}_r , i.e. which are parallel to vector $\mathbf{k}_1 = [r_s, -r_r - r_s, r_r]^T$, do not influence the output velocities $\mathbf{y} = [\omega_s, \omega_c, \omega_r]^T$. Moreover, all the output velocities \mathbf{y} that can be obtained from (11) are perpendicular to vector \mathbf{k}_1 , i.e. the vector \mathbf{y} satisfies the relation:

$$\mathbf{k}_1^T \mathbf{y} = 0 \quad \rightarrow \quad r_s \omega_s - (r_r + r_s) \omega_c + r_r \omega_r = 0.$$

A second dissipative static model can be obtained from the elastic model (9) when $K_{sc} = K_{sc} = \infty$ and $J_p = 0$, that is when $\tilde{\mathbf{L}}_e = 0$:

$$\tilde{\mathbf{x}} = \tilde{\mathbf{A}}_e^{-1} \tilde{\mathbf{B}}_e \tilde{\mathbf{u}}, \quad \rightarrow \quad \tilde{\mathbf{y}} = \mathbf{D}_{s2} \tilde{\mathbf{u}} = (\mathbf{C}_e \tilde{\mathbf{A}}_e^{-1} \tilde{\mathbf{B}}_e + \mathbf{D}_e) \tilde{\mathbf{u}}. \quad (12)$$

Also matrix \mathbf{D}_{s2} is singular and therefore all the velocity vectors $\tilde{\mathbf{u}} = [\omega_s, \omega_c, \omega_r]^T$ which belong to the kernel of matrix \mathbf{D}_{s2} , i.e. which are parallel to vector $\mathbf{k}_2 = [r_s, -r_r - r_s, r_r]^T$, do not influence the output torques $\tilde{\mathbf{y}} = [\tau_s, \tau_c, \tau_r]^T$. Moreover, all the output torques $\tilde{\mathbf{y}}$ that can be obtained from (12) are perpendicular to vector \mathbf{k}_2 , i.e. the vector $\tilde{\mathbf{y}}$ satisfies the relation:

$$\mathbf{k}_2^T \tilde{\mathbf{y}} = 0 \quad \rightarrow \quad r_s \tau_s - (r_r + r_s) \tau_c + r_r \tau_r = 0.$$

IV. POG MODELING OF AN HYBRID AUTOMOTIVE SYSTEM

The planetary gear is the key element for modeling the hybrid powertrain structure shown in Fig. 10. The considered structure includes an internal combustion engine (ICE) and a multi-phase Permanent Magnet Synchronous Machine (PMSM). The planetary gear is the element connecting the two motors and the driving wheels. The ICE is rigidly connected to the Carrier (C), the PMSM is connected to the Sun (S) and the vehicle driving axle is connected to the Ring (R). This hybrid system can be dynamically described by the “high level” POG block scheme shown in Fig. 11. Note that the

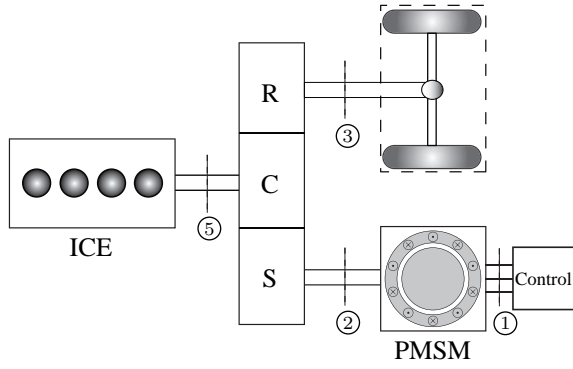


Figure 10. Scheme of the considered power structure of the vehicle

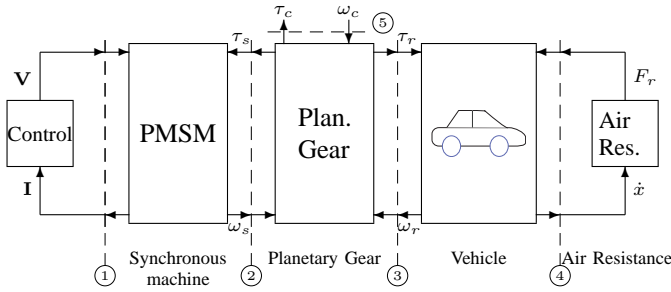


Figure 11. POG graphical representation of the considered hybrid vehicle.

POG power sections ①- ⑤ shown in Fig. 11 correspond to the physical power sections indicated in Fig. 10. The POG block “Control” of Fig. 11 represents the electric control of the PMSM. The POG model of the synchronous machine present between sections ① and ② is given in Fig. 12, see [4] and [5]. The POG model of the Planetary Gear present between sections ② and ③ is given in Fig. 7. The corresponding POG reduced model proposed in Sec. III can also be used. The planetary gear is connected to the driving shaft of the vehicle. The dynamics of the vehicle is described by the POG block present between sections ③ and ④: the details of this POG block can be found in [6]. Finally the resistance of the air is described by the last POG block.

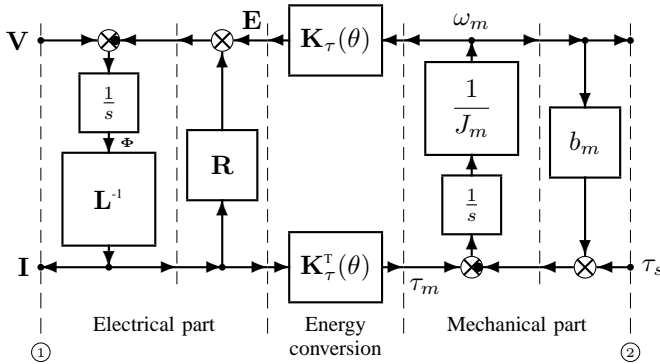


Figure 12. POG scheme of the multi-phase synchronous motor (PMSM).

V. SIMULATION

The system shown in Fig. 10 has been implemented in Matlab/Simulink as it is shown in Fig. 13. All subsystems have been modeled with POG and in particular the vehicle subsystem in the right part of the scheme is a bicycle model of a car that includes the tire-road elastic interaction, see [6].

A full set of simulation results of the controlled hybrid system will be given in the final version of the paper.

REFERENCES

- [1] R. Zanasi, “Power Oriented Modelling of Dynamical System for Simulation”, IMACS Symp. on Modelling and Control of Technological System, Lille, France, May 1991.
- [2] Zanasi R., “Dynamics of a n -links Manipulator by Using Power-Oriented Graph”, *SYROCO '94*, Capri, Italy, 1994.
- [3] D. C. Karnopp, D.L. Margolis, R. C. Rosenberg, *System dynamics - Modeling and Simulation of Mechatronic Systems*, Wiley Interscience, ISBN 0-471-33301-8, 3rd ed. 2000.
- [4] R. Zanasi, F. Grossi, “Multi-phase Synchronous Motors: POG Modeling and Optimal Shaping of the Rotor Flux”, *ELECTRIMACS 2008*, Québec, Canada, June 2008.
- [5] R. Zanasi, F. Grossi “Optimal Rotor Flux Shape for Multi-phase Permanent Magnet Synchronous Motors”, *International Power Electronics and Motion Control Conference*, September 1-3 2008, Poznan, Poland.
- [6] F. Grossi, W. Lhomme, R. Zanasi, A. Bouscayrol, “Modelling and control of a vehicle with tire-road interaction using POG and EMR formalisms”, accepted to *Electromotion 2009*, EPE chapter Electric Drives, 1-3 July 2009, Lille, France

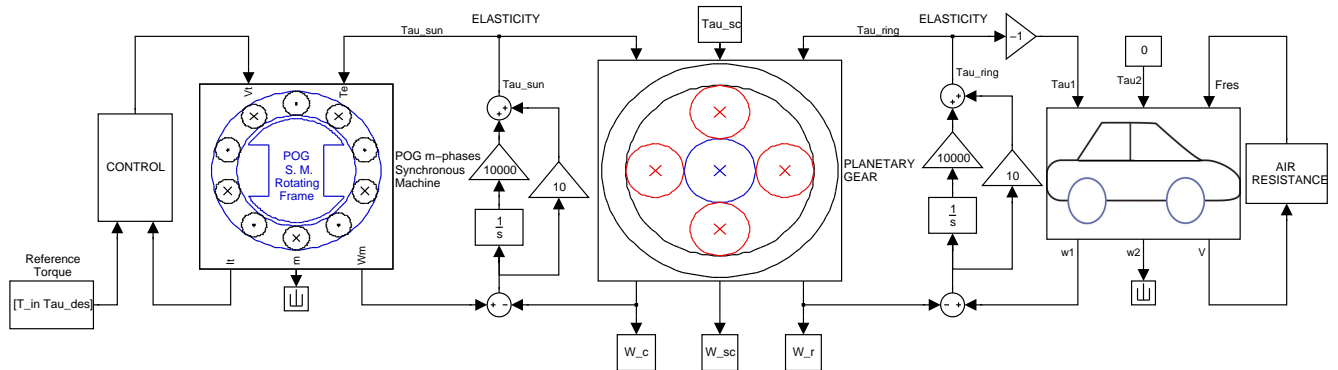


Figure 13. Simulink block scheme of the considered hybrid power structure.